Proteasomal conformation controls unfolding ability

Julianna R. Cresti[a,1], Abramo J. Manfredonia[a,1], Christopher E. Bragança[a], Joseph A. Boscia IV[a], Christina M. Hurley[a], Mary D. Cundiff[a], and Daniel A. Kraut[a,2]

[a]Department of Chemistry, Villanova University, Villanova, PA 19085

Edited by Wolfgang Baumeister, Max Planck Institute of Biochemistry (MPG), Martinsried, Germany, and approved April 29, 2021 (received for review January 17, 2021)

The 26S proteasome is the macromolecular machine responsible for the bulk of protein degradation in eukaryotic cells. As it degrades a ubiquitinated protein, the proteasome transitions from a substrate-accepting conformation (s1) to a set of substrate-processing conformations (s3 like), each stabilized by different intramolecular contacts. Tools to study these conformational changes remain limited, and although several interactions have been proposed to be important for stabilizing the proteasome's various conformations, it has been difficult to test these directly under equilibrium conditions. Here, we describe a conformationally sensitive Förster resonance energy transfer assay, in which fluorescent proteins are fused to Sem1 and Rpn6, which are nearer each other in substrate-processing conformations than in the substrate-accepting conformation. Using this assay, we find that two sets of interactions, one involving Rpn5 and another involving Rpn2, are both important for stabilizing substrate-processing conformations. Mutations that disrupt these interactions both destabilize substrate-processing conformations relative to the substrate-accepting conformation and diminish the proteasome's ability to successfully unfold and degrade hard-to-unfold substrates, providing a link between the proteasome's conformational state and its unfolding ability.

proteasome | protein unfolding | protein degradation | ATP-dependent protease | ATPases associated with diverse cellular activities (AAA)

The 26S proteasome is a molecular machine that is responsible for regulated protein degradation in eukaryotic cells (1). The proteasome is a large multiprotein complex, divided between the 19S regulatory particle, which recognizes ubiquitinated substrates and unfolds them, and the barrel-like 20S core particle, whose interior is lined with protease active sites that degrade the unfolded substrate polypeptide.

The proteasome is dynamic, and multiple conformations have been identified in cryogenic electron microscopy (cryo-EM) structures of free and substrate-engaged proteasomes (2–6). Before substrate recognition and binding, the proteasome is found in the s1 or substrate-accepting state. The ubiquitin chains on the substrate are bound by ubiquitin receptors on the 19S regulatory particle, after which an unstructured initiation region of the substrate enters the pore of the AAA^+ motor (7). The substrate is translocated further into the structure, driven by interactions with aromatic paddle–containing pore loops on a ring of motor proteins, called Rpt1-6, until it is fully engaged; this process triggers a conformational change to a series of substrate-translocating states represented in structures as states s3 to s6 (2). These s3-like states can also be triggered by the nonhydrolyzable ATP analog ATP-γS. In these translocating states, the 19S pore coaxially aligns with the deubiquitinase Rpn11 and the opening to the 20S particle, allowing the substrate to be deubiquitinated, unfolded, translocated into the core particle, and degraded. An s2 state, in which only Rpn11 aligns with the 20S core, has also been seen in the absence of substrate but is not thought to be competent to engage substrates (1).

We have previously shown that the binding of polyubiquitinated substrates to the proteasome activates the proteasome's unfolding ability, the ability to successfully unfold and degrade a substrate, and that this activation is mediated by proteasomal ubiquitin receptors (8, 9). One potential mechanism for this activation would be by inducing or reinforcing the conformational change from the s1 state to s3-like states, as it is likely that productive unfolding requires the proteasome to stay in s3-like states during the entire translocation and degradation process. We thus reasoned that proteasomal interactions that specifically stabilize s3-like states might also be important for proteasomal unfolding ability, and destabilizing s3-like states would reduce unfolding ability.

Interactions between Rpn5 (on the lid of the 19S) and the Rpt3/Rpt4 coiled coil (part of the base of the 19S) are important for conformational switching (10, 11). Specifically, Rpn5 125 to 131 contact Rpt3 in the s1 state of the proteasome but not in s3-like states, while Rpn5 198, 201, and 205 contact Rpt3 and Rpt4 in s3-like states but not in the s1 state (12) (Fig. 1 *A* and *B*). Disrupting the s1 contacts affects proteasome assembly and prevents degradation initiation but leaves later s3-based steps of degradation, including unfolding, unaffected (10, 11). Disrupting the s3 contacts has no impact on proteasome assembly, and polyubiquitin conjugates accumulated in a mutant cell line, suggesting some inhibition of activity (10), but there has been no characterization of the direct effects on the proteasome's unfolding ability. We had also previously noted an interaction within the base of the 19S between Rpn2 R809 and Rpt2 E72 in s3-like states that is replaced by an interaction between Rpn2 R813 and Rpt2 E72 in the s1 state (9, 12) (Fig. 1 *C* and *D*). We

Significance

In eukaryotic cells, the proteasome is responsible for most protein degradation. Because of this central role, the proteasome is of interest in diseases ranging from cancer to neurodegeneration. The proteasome undergoes ATP hydrolysis–driven conformational changes during its catalytic cycle that are important for its activity. In this work, we established a system to use Förster resonance energy transfer to characterize these conformational changes. We show that previous predictions of protein interactions that alter equilibria between resting and active forms of the proteasome are correct, and accessing those active conformations allows the proteasome to better unfold and degrade hard-to-degrade substrates. These results suggest that controlling the proteasome's conformation might be a regulatory strategy to be exploited in drug design.

Author contributions: D.A.K. designed research; J.R.C., A.J.M., C.E.B., J.A.B., and D.A.K. performed research; J.A.B., C.M.H., and M.D.C. contributed new reagents/analytic tools; J.R.C., A.J.M., C.E.B., and D.A.K. analyzed data; and J.R.C., A.J.M., and D.A.K. wrote the paper.

The authors declare no competing interest.

This article is a PNAS Direct Submission.

[1]J.R.C. and A.J.M. contributed equally to this work.

[2]To whom correspondence may be addressed. Email: daniel.kraut@villanova.edu.

This article contains supporting information online at https://www.pnas.org/lookup/suppl/doi:10.1073/pnas.2101004118/-/DCSupplemental.

Published June 14, 2021.

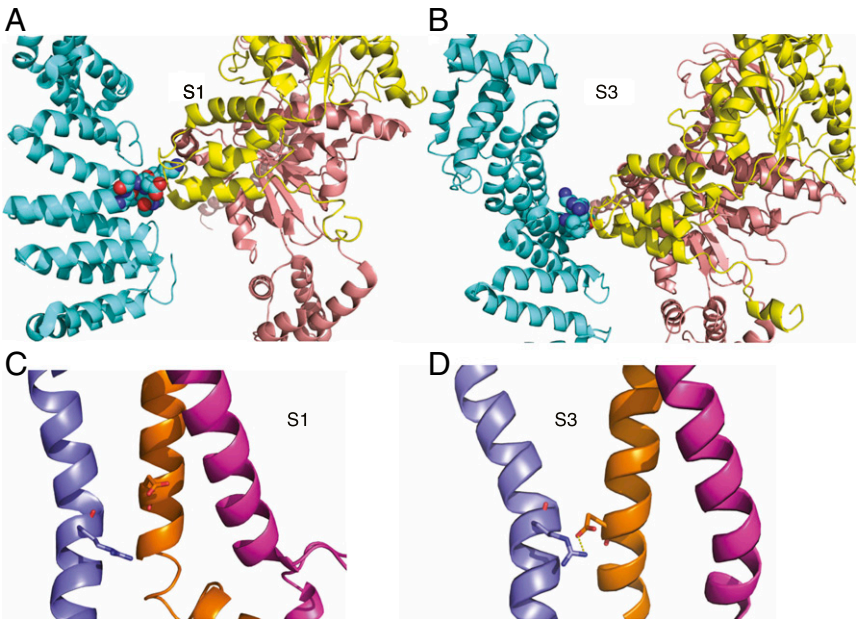

Fig. 1. Proteasomal conformational changes lead to changing interaction surfaces. (*A*) Rpn5 (cyan) residues 125 to 131 (shown as spheres) interact with Rpt3 (yellow) in the s1 conformation. (*B*) Rpn5 (cyan) residues 198, 201, and 205 (shown as spheres) interact with Rpt3 (yellow) and Rpt4 (brown) in the s3 conformation. (*C*) Rpn2 (purple) interacts with the Rpt1 (magenta)/Rpt2 (orange) coiled coil in the s1 conformation, but there is no interaction observed between Rpn2 R809 and Rpt2 E72 (sticks). (*D*) Rpn2 (purple) interacts with the Rpt1 (magenta)/Rpt2 (orange) coiled coil via an Rpn2 R809–Rpt2 E72 interaction in the s3 conformation. Structures are from the Protein Data Bank (PDB), ID 5mp9 (s1) and 5mpb5 (s3).

therefore sought to characterize the effects of destabilizing s3-like states on both the conformation and unfolding ability of the proteasome.

While several methods have been used to examine proteasomal conformation, a sensitive means of easily determining conformations of native proteasomes in solution is lacking. Cryo-EM is not a true solution technique and has extensive technical requirements. Proximity-based cross-linking, although useful, isn't a true equilibrium approach (2, 13). Förster resonance energy transfer (FRET) is an ideal technique, as it is sensitive to small distance changes and allows for real-time detection so that it can be used for both equilibrium and kinetic measurements. However, FRET requires site-specific labeling, which for the proteasome requires unnatural amino acid incorporation and proteasomal reconstitution, which is expensive and technically challenging (14, 15). Herein, we develop a FRET-based assay to monitor the conformation of natively expressed yeast proteasome and examine the effects of s3-destabilizing mutants on the unfolding ability of the proteasome.

Results

Dual-Labeled Proteasome Has Conformationally Sensitive FRET. We reasoned that conformationally sensitive FRET would be possible using endogenously expressed yeast proteasome if appropriate fluorescent proteins were appended to otherwise wild-type (WT) proteasome subunits. The distance between the C terminus of Sem1 and the N terminus of Rpn6 decreases from 94 Å in the s1 substrate-accepting conformation to only ∼80 Å apart in the s2 to s6 conformations (Fig. 2 *A* and *B* and Table 1) (2). A similar shortening between Sem1 and Rpn6 is seen comparing the Ub-accepted state (∼99 Å) and the Ub-engaged state (∼81 Å) observed by Ding et al. and comparing the substrate-accepting and substrate-processing states of the human proteasome described by Dong et al. (4, 5). We chose to fuse mTurquoise (mTq) (16) to the C terminus of Sem1 as a FRET donor and mNeonGreen (mNG) (17) to the N terminus of Rpn6 as an FRET acceptor. mTq/mNG FRET pairs have high efficiency and have an R_0 of ∼62 Å, making them suitable for distance changes in the ∼40 to 90 Å range (18). mTq has maximal emission at ∼474 nm, while mNG has maximal excitation at 506 nm and maximal emission at 517 nm. DNA encoding the fluorophores was integrated into the yeast genome using CRISPR-Cas9. The resulting yeast were viable and grew normally; fluorescence levels were low enough that the yeast was not visibly fluorescent, consistent with fluorescent proteins being expressed at endogenous levels. Affinity-purified proteasome contained two fluorescent bands consistent in size with Sem1-mTq and mNG-Rpn6 (Fig. 2*C*), and native gel analysis indicated that proteasome was intact, retained peptidase activity, and was fluorescent (Fig. 2*D*). WT FRET-labeled proteasome (WT_{FRET}) was also active in the degradation of ubiquitinated protein substrates, with degradation rates within twofold of WT and unfolding ability (a measure of proteasomal processivity; see *Mutations that Perturb Proteasomal Conformation Decrease Unfolding Ability*) indistinguishable from WT (*SI Appendix*, Fig. S1).

Comparing the spectrum of purified WT_{FRET} proteasome with that of proteasome containing only the donor fluorescent protein Sem1-mTq (WT_{Donor}), FRET induces a new peak at ∼512 nm (Fig. 3*A*). Direct excitation of mNG is minimal at our chosen excitation wavelength (400 nm; Fig. 3*A*), so we attribute this increased fluorescence to an FRET signal from mNG. Replacement of ATP with the nonhydrolyzable ATP analog ATP-γS, which has previously been shown to shift the proteasome from a mixture of s1 and s2 states to predominantly s3 to s5 states (2), led to a further increase in this FRET signal for WT_{FRET} proteasome but had no effect on WT_{Donor} proteasome (Fig. 3*A*). We therefore used the ratio of these two peaks (F_{512}/F_{474}) to quantify relative changes in FRET, with decreases in FRET indicating shifts toward the s1 state and increases indicating shifts toward processing states.

We next examined the effects of mutations predicted to perturb the proteasome's conformational equilibria on FRET levels.

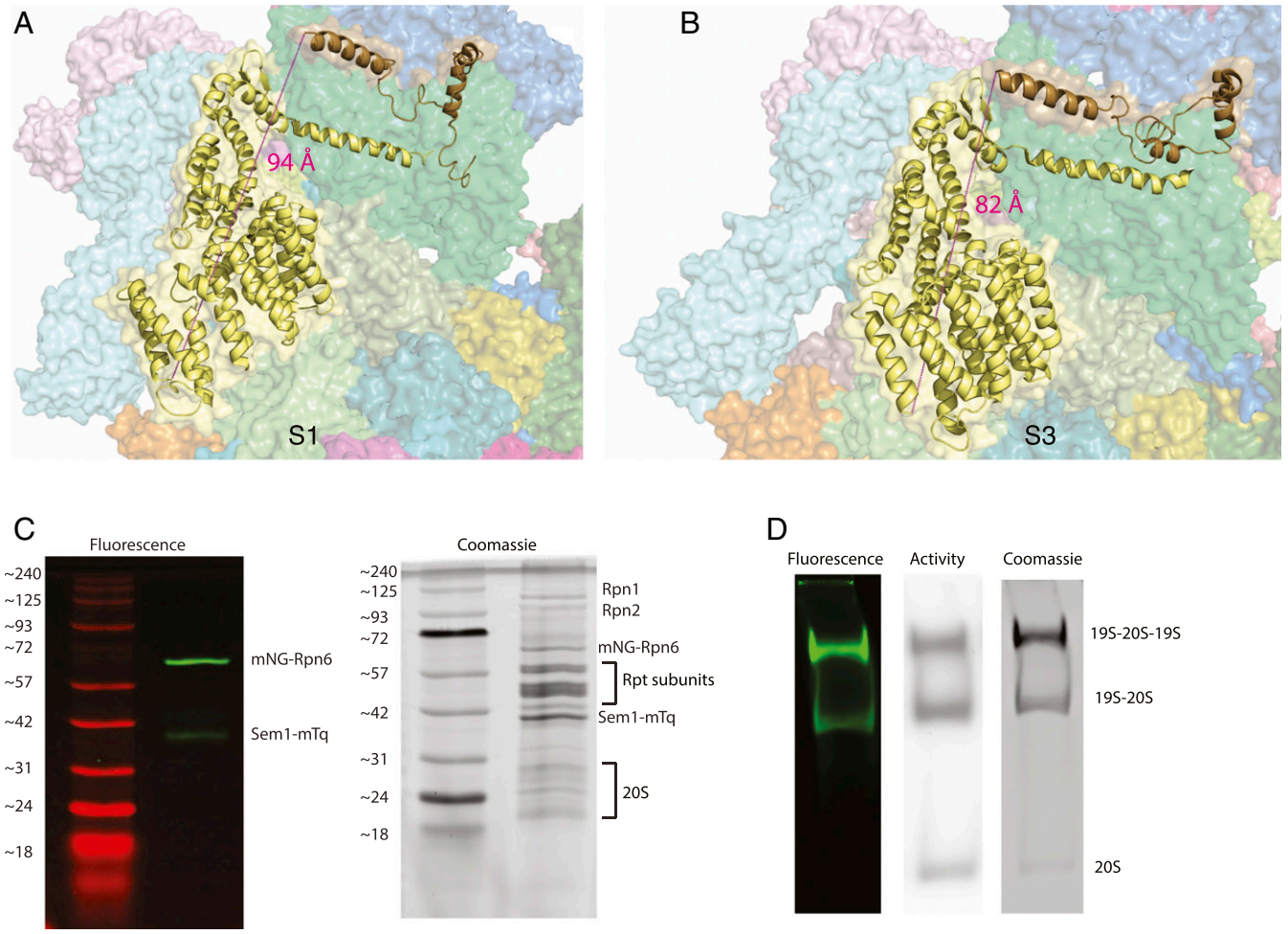

Fig. 2. Design of FRET-labeled proteasome, with fluorescent proteins fused to the C terminus of Sem1 and the N terminus of Rpn6. (*A*) Distance between Sem1 Gln89 and Rpn6 Met1 in the s1 state is 94 Å (PDB ID 6FVT). (*B*) Distance between Sem1 Gln89 and Rpn6 Met1 in the s3 state is 82 Å (PDB ID 6FVV). (*C*) SDS-polyacrylamide gel electrophoresis of FRET-labeled proteasome, imaged by fluorescence (excitation at 473 nm) or by Coomassie staining. (*D*) Native gel of FRET-labeled proteasome, imaged by fluorescence (excitation at 473 nm), Suc-LLVY-AMC activity assay, or by Coomassie staining.

Mutating the residues in Rpn5 that contact Rpt3 and Rpt4 (Fig. 1*B*) has previously been predicted to bias the proteasome against s3-like states and caused the accumulation of polyubiquitinated proteins in vivo (10). Indeed, an Rpn5-s3mut FRET-labeled proteasome (Rpn5 V198W/R201F/K205A) showed decreased FRET levels in the presence of ATP (Fig. 3 *B* and *C*), consistent with a shift toward the s1 or s1-like states. The addition of ATP-γS still increased FRET, but FRET levels were lower than with WT_{FRET}, indicating that the equilibrium is perturbed away from s3-like states. Similarly, the R809E mutation to Rpn2 (Rpn2-s3mut), which contacts Rpt2 in the s3 state, decreased FRET levels in the presence of ATP-γS (Fig. 3 *B* and *C*). The slight decrease in FRET for Rpn2-s3mut in the presence of ATP was not statistically significant. Proteasome conformational changes reorient the ATPase subunits and thus can affect ATPase activity. Rpn5-s3mut's ATPase activity was reduced by more than twofold, while Rpn2-s3mut saw a smaller increase in ATPase activity, which, along with the differences in FRET effects, suggests somewhat different mechanisms of action for the two mutations (Fig. 3*D*).

Table 1. Distances between Sem1 (C-terminal Gln89) and Rpn6 (Met1)

PDB ID	Conformation	Distance (Å)
6fvt	s1	94.2
6fvu	s2	82.4
6fvv	s3	81.8
6fvw	s4	80.3
6fvx	s5	79.8
6fvy	s6	83.1

Mutations that Perturb Proteasomal Conformation Decrease Unfolding Ability. We next examined the effect of these s3-state disfavoring mutations on the proteasome's ability to unfold and degrade substrates. After ubiquitinated substrates bind to the proteasome, the substrate is engaged by the proteasomal motors and deubiquitinated, and it is believed that this activation correlates with a shift into s3-like processing conformations. Thus, destabilizing the s3 state might be predicted to decrease the proteasome's unfolding ability if the proteasome can transition back to the s1 state while trying to translocate and unfold a substrate. We made Rpn5-s3mut and Rpn2-s3mut in a non-FRET background and examined their ability to unfold and degrade a model substrate we have previously used to quantitatively determine the proteasome's unfolding ability (9) (Fig. 4*A*). Briefly, an N-terminal degron derived from Nrf2 (Neh2Dual) is followed by an easy-to-unfold barnase domain

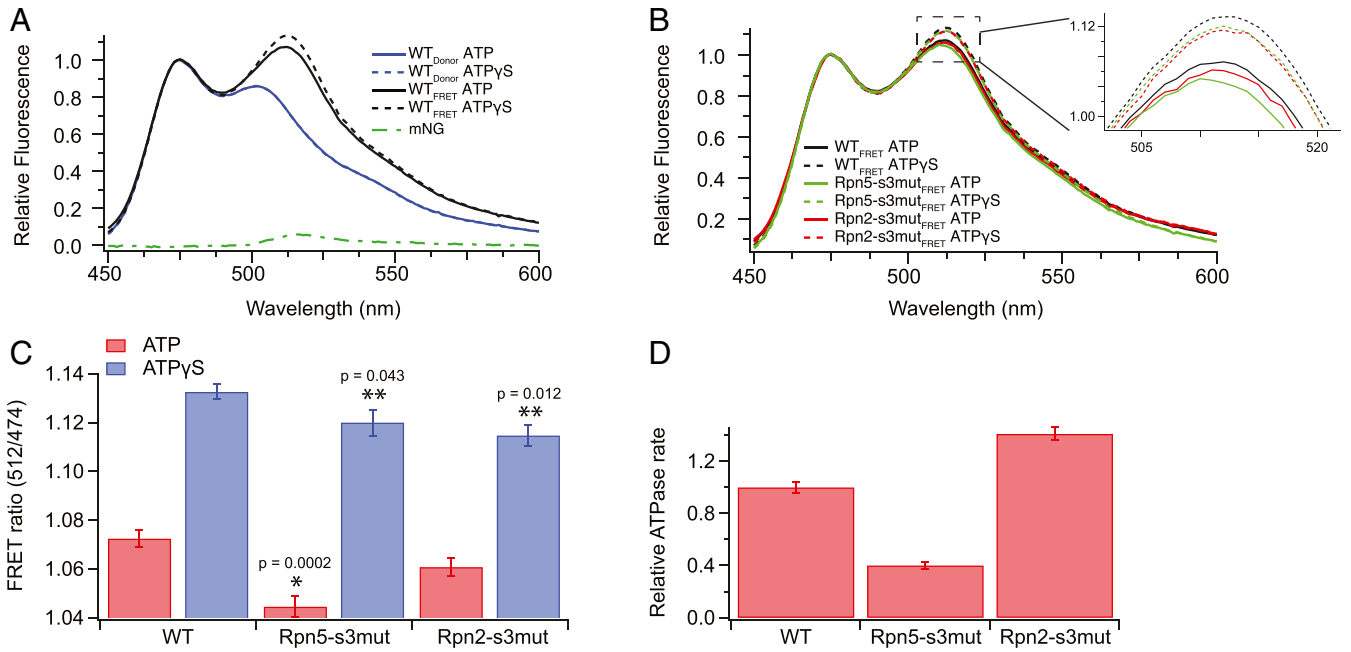

Fig. 3. FRET depends on proteasome conformation. (*A*) Fluorescence spectra of labeled proteasomes, with excitation at 400 nm. The spectrum of 20 nM Sem1-mTq/mNG-Rpn6 proteasome (WT_{FRET}; black) increases in mNG fluorescence (peak at 512 nm) upon the addition of ATP-γS (dashed versus solid lines). There is no effect of ATP-γS on proteasome containing the donor fluorophore (Sem1-mTq) only (WT_{Donor}; blue). The spectrum of 20 nM mNG directly excited at 400 nm is shown for comparison (green). All spectra were normalized to the mTq peak of 474 nm, except for mNG, which is scaled relative to the intensity of WT_{FRET}ATP at 474 nm. The average of 3 to 12 experiments are shown. (*B*) Fluorescence spectra of WT_{FRET} and mutant proteasomes in the presence of ATP or ATP-γS, as in *A*. The *Inset* shows the 512-nm peak. The average of 3 to 12 experiments are shown. (*C*) FRET ratios (fluorescence at 512 nm divided by fluorescence at 474 nm) for spectra from *B*. Two-tailed *t* tests were used to determine significant differences from WT in the presence of ATP (*) or ATP-γS (**). (*D*) Relative ATPase rates for WT and mutant proteasome.

and a more difficult to unfold dihydrofolate reductase (DHFR) domain, which is further stabilized by the addition of NADPH. The degron is ubiquitinated with branched K48- and K63-containing chains using the Keap1/Cul3/Rbx1 E3 ligase; all nondegron lysines, except a single lysine in DHFR, have been replaced, and ubiquitination in the presence of NADPH prevents ubiquitination of the DHFR domain (9). The construct contains a single cysteine between barnase and DHFR, which is labeled with Cy5 for fluorescent detection. After encountering the degron, removing ubiquitin, and unfolding and degrading the barnase domain, the proteasome will partition between successful unfolding and degradation of DHFR and irreversible release of a DHFR-containing fragment (8, 9, 19). The unfolding ability (U) is defined as the ratio of the rate of unfolding and degradation to the rate of release and can be determined from the amount of DHFR fragment formed relative to the amount of full-length protein degraded:

$$U = \frac{k_{frag}^{deg}}{k_{frag}^{rel}} = \frac{Amplitude\ Full\text{-}length\ Degradation - Amplitude\ Fragment\ Formation}{Amplitude\ Fragment\ Formation} = \frac{Amplitude\ Complete\ Degradation}{Amplitude\ Fragment\ Formation}. \quad [1]$$

Rpn5-s3mut showed a markedly lower rate of degradation than WT proteasome (v_0 = 0.6 ± 0.2% min^{-1} versus 9 ± 1% min^{-1}), while Rpn2-s3mut degraded the full-length substrate at a similar rate to WT (12 ± 1% min^{-1}) (Fig. 4 *B–D*). Deubiquitination of the substrate was not observed with either WT or the mutants. Both Rpn5-s3mut and Rpn2-s3mut increased the fraction of full-length substrate that was released as a partially degraded DHFR-containing fragment instead of being completely degraded, indicating that both mutations decrease the unfolding ability of the proteasome (Fig. 4*E*). For both mutants and WT, degradation was due to the proteasome, as proteasome inhibitors efficiently prevented both degradation and DHFR fragment formation (*SI Appendix*, Fig. S2). Degradation was also ubiquitin dependent, as linear K48-linked polyubiquitin chains slowed degradation, presumably by competing for ubiquitin receptors (*SI Appendix*, Fig. S3). Interestingly, the mutants were inhibited by K48-linked chains to a lesser extent than was WT, suggesting that either ubiquitin chain linkage preferences are changed by conformational mutants (the substrate contains branched chains, while the inhibitor was linear) or bias toward s1-like states enhances substrate binding. Proteasome mutants are still capable of degrading easier-to-unfold substrates, as in the absence of NADPH to stabilize DHFR; the conformational mutants are able to completely degrade the substrate without forming any stable fragments (*SI Appendix*, Fig. S4). Unfolding abilities did not differ because of differences in proteasome assembly, as all mutants were able to assemble into 26S proteasome (*SI Appendix*, Fig. S5), and the residual 19S present in some proteasome preps did not affect the unfolding ability (*SI Appendix*, Fig. S6).

To test whether and how the degradation of other substrates was impaired by mutations that perturb the proteasome's conformational equilibrium, we examined the degradation of GFP-containing substrates targeted to the proteasome via an N-terminal ubiquitin-like (UBL) domain. We previously showed that UBL-sGFP-102-His_6 is degraded from the C-terminal unstructured initiation region, and degradation proceeds through an intermediate that can be released and rebound (20) (Fig. 5*A*, blue). At the same time, UBL-independent but proteasome-dependent

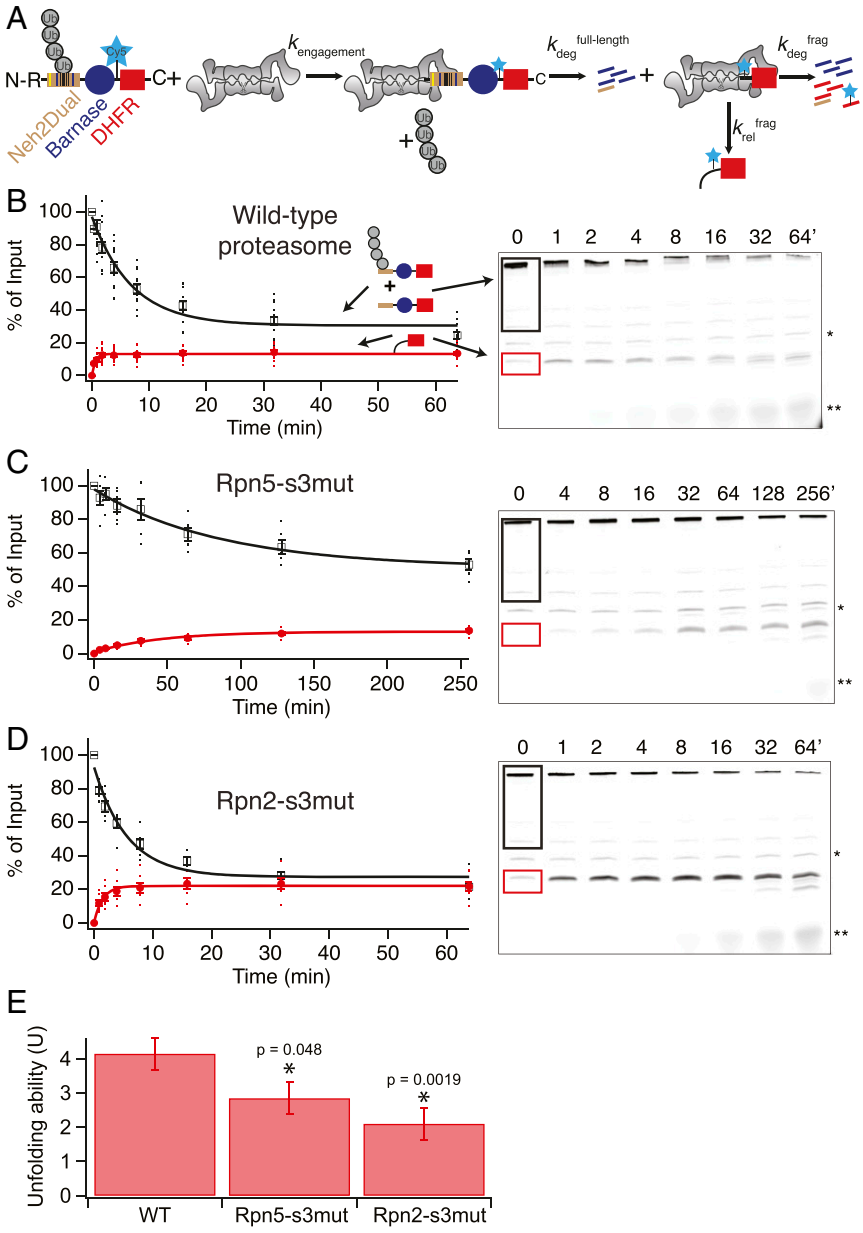

Fig. 4. Proteasome conformational mutants decrease the unfolding ability of the proteasome. (*A*) Unfolding ability assay, in which a substate is engaged by the proteasome ($k_{engagement}$), barnase is unfolded and degraded ($k_{deg}^{full\text{-}length}$), and then DHFR is either degraded (k_{deg}^{frag}) or irreversibly released (k_{rel}^{frag}); the ratio of these two rate constants gives the unfolding ability (U). (*B–D*) Degradation of 20 nM ubiquitinated Neh2Dual-BarnaseΔK-Cy5-DHFRδKΔC by 100 nM WT (*B*), Rpn5-s3mut (*C*), or Rpn2-s3mut (*D*) proteasome. Black box shows the region of the gel containing full-length protein with or without ubiquitination. Red box shows the region of the gel containing the DHFR fragment. The amounts of full-length protein (open squares) and DHFR fragment (red circles) are shown as a percentage of the ubiquitinated full-length substrate presented to the proteasome at the beginning of the reaction; the full-length protein is quantified as the sum of ubiquitinated and nonubiquitinated full-length species so any deubiquitination is not misinterpreted as degradation. Dots are results from individual experiments, and error bars represent the SEM of 15 (*A*), 7 (*B*), or 6 (*C*) experiments. Curves are global fits to single exponentials. Sample gels (scanned for Cy5 fluorescence) are shown on the right. * marks a contaminant in the substrate that is not ubiquitinated or degraded, and ** marks dye-labeled peptides that are degradation products when DHFR is completely degraded. (*E*) Unfolding abilities (U) calculated from the curve fits shown in *B–D*, according to Eq. 1. Error bars are the SEM propagated from curve fitting the collected datasets. Two-tailed *t* tests were used to determine significant differences from WT (*).

clipping can result in a shorter GFP-containing fragment that can no longer be degraded by the proteasome (Fig. 5*A*, purple), but this happens infrequently (~10% of the time) with WT proteasome. Slowing the rate of GFP unfolding increases the extent to which nonproductive clipping occurs (20). In contrast, replacing sGFP with a circular permutant that is easier to unfold (cp8sGFP) leads to degradation with no detectable nonproductive clipping (Fig. 5*B*).

Rpn5-s3mut showed a dramatic decrease in degradation and an increase in nonproductive clipping (Fig. 5 *C* and *G*) with the sGFP-containing substrate. Rpn5-s3mut could still degrade the cp8sGFP-containing substrate, albeit to a lesser extent than WT (Fig. 5*D*). There may have been some GFP-containing fragment formed, but with this substrate, the fragment band was not distinct enough from the full-length substrate to quantify. Rpn2-s3mut had a more modest unfolding defect with the sGFP-containing substrate and

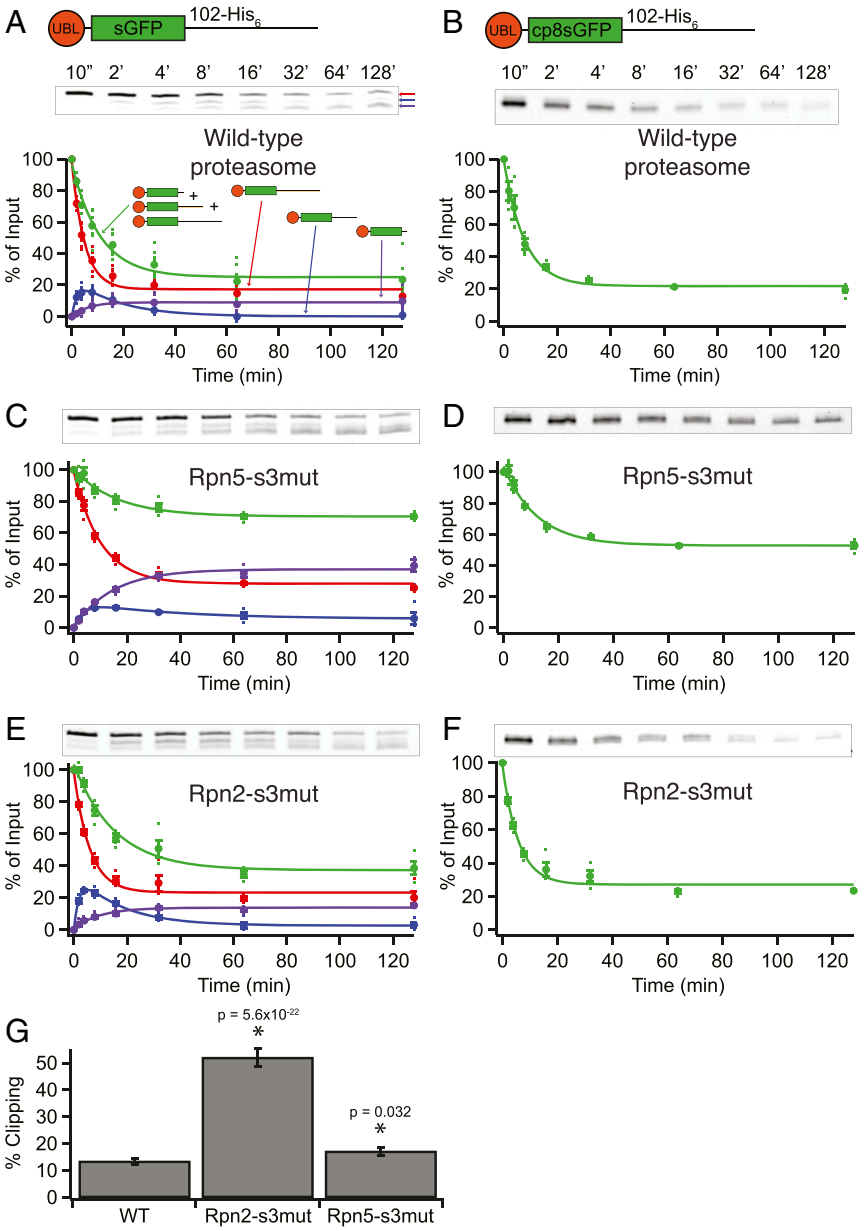

Fig. 5. Proteasome conformational mutants increase the clipping of sGFP-containing substrates. (*A* and *B*) Degradation of 100 nM UBL-sGFP-102-His_6 (*A*) or 100 nM UBL-cp8-sGFP-102-His_6 (*B*) by 100 nM WT yeast proteasome. Representative gel shows the disappearance of full-length protein (red arrow) and the appearance of longer (blue arrow) and shorter (purple arrow) clipped protein. The amounts of full-length protein (red circles), longer partially degraded protein (blue circles), shorter clipped protein (purple circles), and total fluorescence (green circles) are shown as a percentage of the full-length substrate presented to the proteasome at the beginning of the reaction. For the cp8 substrate, minimal clipped protein was formed, so only the disappearance of total fluorescence is quantified. Dots are results from individual experiments, and error bars represent the SEM of 8 and 14 experiments, respectively. Curves are global fits to single exponentials. Data from ref. 20. (*C–F*) The same as in *A* and *B* but for proteasome mutants. Error bars represent the SEM of four experiments. (*G*) Percentage of full-length, sGFP-containing protein that was clipped (formed a smaller fragment) rather than being degraded. Two-tailed *t* tests were used to determine significant differences from WT (*).

no observable defect with the cp8sGFP-containing substrate (Fig. 5 *E–G*). Michaelis–Menten analysis of these substrates under multiple turnover conditions indicates that although Rpn5-s3mut's ability to turn over the substrate (presumably limited by unfolding) is greatly reduced, there is no effect on binding, as all three proteasomes have a K_M of ~100 nM, similar to previous reports of UBL–proteasome affinity (21) (*SI Appendix*, Fig. S7). Thus, conformational mutants slow the unfolding and degradation of substrates targeted to the proteasome via either UBL or ubiquitin modifications, especially for the hardest-to-unfold substrates.

Discussion

The proteasome functions by cycling through a series of conformations as it binds to, engages, unfolds, and translocates proteins destined for degradation into the 20S core particle. Herein, we describe a FRET-based tool to probe the conformation of the proteasome that is complementary to existing fluorescence, cross-linking, and structural methods. By using this tool, we have confirmed that Rpn5 residues that contact the Rpt3/Rpt4 coiled coil in s3-like states are indeed important for stabilizing the s3 conformation, as their mutation causes a

decrease in FRET in both the "resting" ATP state and the "engaged" ATP-γS state of the proteasome. It has been shown previously that in the presence of ATP, the proteasome is present in a mixture of s1 and s2 conformations (2); it therefore seems likely that this equilibrium is shifted toward the s1 state upon mutation, as the s2 conformation has a FRET distance similar to that of the s3 conformation (Table 1). In the presence of ATP-γS, a variety of states have been observed (principally s3 to s5, although there is a small s1 population as well). Reduced FRET in the presence of ATP-γS likely indicates a shift in equilibrium toward the s1 state. We cannot rule out a shift between different s3-like states, though these should have very similar distances between our FRET probes (Table 1). These conformational shifts have functional consequences, as Rpn5-s3mut proteasome degrades substrates much more slowly than WT proteasome and is more likely to stall while unfolding and therefore prematurely releases the substrate.

Similarly, disrupting an s3-like, state-specific contact between Rpn2 and Rpt2 showed reduced FRET in the presence of ATP-γS, most likely indicating a shift toward the s1 state. Although the effects of the Rpn2-s3mut mutation were less severe overall than those of the Rpn5-s3mut mutation (smaller drop in FRET in the presence of ATP and smaller effects on overall degradation rates), there was also a marked decrease in proteasomal processivity or unfolding ability. The difference in the magnitude of the effects of mutation could be due to a less extensive or less well-ordered interface, as some recent cryo-EM structures have this region of Rpn2 visible, and others do not. Of the structures that do exist, the nature of the interaction between Rpn2 and Rpt2 is inconsistent. For example, in a recent structure, Rpn2 R809 interacts with Rpt1 D58, not Rpt2 E72 (2). Additional structural information could be used to more incisively disrupt this interaction in the s3 state, or FRET could be used to screen for additional residues that contribute to this interface. It is also possible that the Rpn2-s3 mutation and the Rpn5-s3 mutation affect different parts of the protein degradation process, with Rpn5-s3 having a larger effect on the early s1/s2 equilibrium and Rpn2-s3 having a larger effect on the balance between s1-like and translocating states. Differential effects would be consistent with the decrease in ATPase activity seen with only Rpn5-s3.

In addition to these equilibrium changes, mutation may also result in kinetic effects on the conformational change process. In particular, if s3-like states are stabilized by interactions between Rpn2 and Rpt2 and Rpn5 and Rpt3/4, weakening these interactions may make it easier for the proteasome to slip back into the s1 state prematurely. Proteasome activation, which we have previously shown involves substrate-linked ubiquitin binding to ubiquitin receptors (8, 9), presumably shifts the proteasome into translocation-competent states, which are capable of unfolding even difficult-to-unfold substrates. If the proteasome makes occasional excursions to the s1 state while trying to unfold a substrate, force cannot be applied efficiently, and the substrate is less likely to be unfolded, potentially allowing the substrate to be prematurely released. The more time the proteasome spends in the s1 state (or the faster it can switch to the s1 state), the more likely unfolding will fail, and a partially degraded fragment will be produced. Single-molecule FRET experiments may be helpful to examine the kinetics of conformational switching and to determine whether such back switching indeed occurs.

Finally, although our experiments dealt with mutations that destabilize translocating states of the proteasome, it seems likely that nature has similarly designed proteasome effectors that bias the proteasome toward one conformational state or another. For example, under stressful conditions such effectors might stabilize the substrate-accepting state at the expense of processivity to allow rapid degradation of weakly folded proteins for whom a high unfolding ability might not be crucial. Small molecules might also be designed to stabilize translocating states of the proteasome and thus increase unfolding ability, perhaps allowing the proteasome to successfully degrade the stably misfolded proteins that are the earliest stages of protein-folding diseases.

Methods

Constructs. A pE-SUMO–based His-SUMO-Neh2-Barnase-Cys-DHFR construct with no lysines in barnase, all cysteines removed, and a Cys-containing linker between barnase and DHFR has been described previously (9). All DHFR lysines, except for K76 (mutation of which destabilized DHFR), were mutated to arginine via oligo-directed mutagenesis to prevent internal ubiquitination of the DHFR domain (9).

Yeast Strains. Yeast mutants were made in the background of strain YYS40 (22), which contains a 3× FLAG-tagged copy of Rpn11 to aid in proteasome purification. WT_{Donor} proteasome was created by CRISPR-based mutagenesis. A Cas9/guide RNA (gRNA) construct (23) targeting Sem1 was cotransformed into YYS40 with a PCR product containing mTq [amplified from pRSET-mTq (16)], with 42 base pairs of homologies to the 3′ end of Sem1 at its 5′ end and 40 base pairs of homology to the 3′ untranslated region (UTR) at its 3′ end. After screening colonies for the correct insert size, DNA was extracted and sequenced to confirm in-frame fusion of mTq, and CRISPR plasmid was removed by treatment with 5-Fluoroorotic acid. WT_{FRET} proteasome was similarly created by cotransforming a Cas9/gRNA construct targeting Rpn6 and an mNG-containing PCR product (17), with homology to the 5′ UTR and 5′ end of Rpn6 into WT_{Donor} yeast. Rpn2 and Rpn5 mutants were also made in either YYS40 or WT_{FRET} backgrounds using CRISPR-based mutagenesis, using Cas9/gRNA constructs targeting appropriate locations in Rpn2 or Rpn5 and rescue oligos encoding the desired mutations. Strains are listed in *SI Appendix*, Table S1.

Proteasome Purification. Proteasome was purified from WT strain YYS40 or mutant strains using a 3× FLAG-tagged copy of Rpn11 subunit of the 19S particle, as described previously (9). All proteasome mutants were confirmed to assemble into 26S particles by native gel analysis (*SI Appendix*, Fig. S5).

Native Gels. Proteasome (~6 μg) was run on a 3.5% native gel and visualized using fluorescence (for FRET-labeled proteasome), activity with Suc-LLVY-AMC in the presence of 0.02% SDS and by Coomassie staining (24).

Fluorescence. A total of 20 nM fluorescently tagged proteasome was incubated at room temperature in assay buffer (50 mM TrisCl, 5 mM $MgCl_2$, 5% glycerol [volume/volume], 1 mg/mL bovine serum albumin [BSA], and 1% DMSO [volume/volume], pH 7.5) in the presence of either an ATP regeneration system (1 mM ATP, 10 mM creatine phosphate, and 0.1 mg · mL^{-1} creatine kinase) or 1 mM ATP-γS. Emission spectra (excitation 400 nm) were then recorded at 20 °C with a FluoroMax Plus-C spectrofluorometer with an integration time of 0.2 s · nm^{-1}. Blanks (lacking proteasome) were subtracted, and data were then normalized to the mTq peak at 474 nm.

ATPase Assays. Proteasome ATPase activity was measured using a coupled pyruvate kinase/lactate dehydrogenase assay in saturating ATP, which can be spectrophotometrically detected at 340 nm. The reactions contained 20 nM FRET-labeled proteasome (normalized via total fluorescence at 474 nm), 6.8 units/mL pyruvate kinase, 9.9 units/mL lactate dehydrogenase, 0.4 mM NADH, 2 mM phosphoenolpyruvate, 0.5 mM DTT, and 0.5 mM ATP in a buffer consisting of 50 mM Hepes-KOH, pH 7.5, 50 mM KCl, and 5 mM $MgCl_2$. The reaction was run at 30 °C in a 384-well plate with time points taken every 20 s for 20 min by a Bio-Rad Benchmark Plus ultraviolet-visible plate reader.

Substrate Purification and Ubiquitination. His-SUMO-Neh2Dual-Barnase-Cys-DHFR was overexpressed, purified, had the SUMO tag removed, was labeled with sulfo-cyanine5 maleimide (Lumiprobe), and was repurified by gel filtration, as described previously (9). Labeled substrate was then ubiquitinated using the Keap1/Cul3/Rbx1 ubiquitination system (9). The reaction contained 130 nM E1, 3 μM UbcH5 (E2), 3 μM Cul3/Rbx1 (E3), 3 μM Keap1 C151S, 5 mM ATP, 1.5 μM substrate, 500 μM NADPH to prevent internal ubiquitination on the one remaining DHFR lysine, and 0.73 mg · mL^{-1} ubiquitin in Keap1 ubiquitination buffer (45 mM TrisCl, 100 mM NaCl, and 10 mM $MgCl_2$, pH 8.0) and was incubated for 2 h at 30 °C. Following ubiquitination, the substrate was purified by spin size exclusion, as described previously (8).

BIOCHEMISTRY

Degradation Assays. Degradation assays with ubiquitinated or UBL-tagged substrates were conducted using 100 nM proteasome and 20 nM fluorescently labeled ubiquitinated substrate or 100 nM GFP-containing substrate over a 1 to 4 h time course, as described previously (20). The reactions were carried out at 30 °C in degradation buffer (50 mM TrisCl, 5 mM $MgCl_2$, 5% [volume/volume] glycerol, 1 mM ATP, 10 mM creatine phosphate, 0.1 mg/mL creatine kinase, 1 mg/mL BSA, and 1% DMSO [volume/volume], pH 7.5). Reactions with DHFR-containing substrate contained 500 μM NADPH to stabilize DHFR unless otherwise indicated. For Michaelis–Menten analysis, assays were conducted at 30 °C in Grenier 384-well, low-binding black plates using 20 nM proteasome and up to 700 nM UBL-tagged GFP substrate, and GFP fluorescence was monitored in a ClarioStar Plus plate reader. Fluorescence versus time was divided by a control-lacking proteasome, and the initial linear portion of the curve was used to determine the initial rate of reaction.

Data Availability. All study data are included in the article and/or *SI Appendix*.

ACKNOWLEDGMENTS. A plasmid-encoding mTq was a gift from Theodorus Gadella. We thank Aimee Eggler for helpful discussions and feedback. This material is based on work supported by the Beckman Scholars Program and the NSF under Grant No. 1935596 to D.A.K.

1. J. A. M. Bard *et al*., Structure and function of the 26S proteasome. *Annu. Rev. Biochem.* **87**, 697–724 (2018).
2. M. R. Eisele *et al*., Expanded coverage of the 26S proteasome conformational landscape reveals mechanisms of peptidase gating. *Cell Rep.* **24**, 1301–1315.e5 (2018).
3. A. H. de la Peña, E. A. Goodall, S. N. Gates, G. C. Lander, A. Martin, Substrate-engaged 26S proteasome structures reveal mechanisms for ATP-hydrolysis-driven translocation. *Science* **362**, eaav0725 (2018).
4. Y. Dong *et al*., Cryo-EM structures and dynamics of substrate-engaged human 26S proteasome. *Nature* **565**, 49–55 (2019).
5. Z. Ding *et al*., Structural snapshots of 26S proteasome reveal tetraubiquitin-induced conformations. *Mol. Cell* **73**, 1150–1161.e6 (2019).
6. S. N. Gates, A. Martin, Stairway to translocation: AAA+ motor structures reveal the mechanisms of ATP-dependent substrate translocation. *Protein Sci.* **29**, 407–419 (2020).
7. H. Yu, A. Matouschek, Recognition of client proteins by the proteasome. *Annu. Rev. Biophys.* **46**, 149–173 (2017).
8. E. L. Reichard *et al*., Substrate ubiquitination controls the unfolding ability of the proteasome. *J. Biol. Chem.* **291**, 18547–18561 (2016).
9. M. D. Cundiff *et al*., Ubiquitin receptors are required for substrate-mediated activation of the proteasome's unfolding ability. *Sci. Rep.* **9**, 14506 (2019).
10. A. A. Nemec, A. K. Peterson, J. L. Warnock, R. G. Reed, R. J. Tomko Jr, An allosteric interaction network promotes conformation state-dependent eviction of the Nas6 assembly chaperone from nascent 26S proteasomes. *Cell Rep.* **26**, 483–495.e5 (2019).
11. E. R. Greene *et al*., Specific lid-base contacts in the 26s proteasome control the conformational switching required for substrate degradation. *eLife* **8**, e49806 (2019).
12. M. Wehmer *et al*., Structural insights into the functional cycle of the ATPase module of the 26S proteasome. *Proc. Natl. Acad. Sci. U.S.A.* **114**, 1305–1310 (2017).
13. R. G. Reed, R. J. Tomko Jr, Engineered disulfide crosslinking to measure conformational changes in the 26S proteasome. *Methods Enzymol.* **619**, 145–159 (2019).
14. J. A. M. Bard, A. Martin, Recombinant expression, unnatural amino acid incorporation, and site-specific labeling of 26S proteasomal subcomplexes. *Methods Mol. Biol.* **1844**, 219–236 (2018).
15. J. A. M. Bard, C. Bashore, K. C. Dong, A. Martin, The 26S proteasome utilizes a kinetic gateway to prioritize substrate degradation. *Cell* **177**, 286–298.e15 (2019).
16. J. Goedhart *et al*., Bright cyan fluorescent protein variants identified by fluorescence lifetime screening. *Nat. Methods* **7**, 137–139 (2010).
17. N. C. Shaner *et al*., A bright monomeric green fluorescent protein derived from Branchiostoma lanceolatum. *Nat. Methods* **10**, 407–409 (2013).
18. M. Mastop *et al*., Characterization of a spectrally diverse set of fluorescent proteins as FRET acceptors for mTurquoise2. *Sci. Rep.* **7**, 11999 (2017).
19. D. A. Kraut *et al*., Sequence- and species-dependence of proteasomal processivity. *ACS Chem. Biol.* **7**, 1444–1453 (2012).
20. C. E. Bragança, D. A. Kraut, Mode of targeting to the proteasome determines GFP fate. *J. Biol. Chem.* **295**, 15892–15901 (2020).
21. H. Yu, G. Kago, C. M. Yellman, A. Matouschek, Ubiquitin-like domains can target to the proteasome but proteolysis requires a disordered region. *EMBO J.* **35**, 1522–1536 (2016).
22. Y. Saeki, E. Isono, A. Toh-E, Preparation of ubiquitinated substrates by the PY motif-insertion method for monitoring 26S proteasome activity. *Methods Enzymol.* **399**, 215–227 (2005).
23. M. F. Laughery *et al*., New vectors for simple and streamlined CRISPR-Cas9 genome editing in Saccharomyces cerevisiae. *Yeast* **32**, 711–720 (2015).
24. S. Elsasser, M. Schmidt, D. Finley, Characterization of the proteasome using native gel electrophoresis. *Methods Enzymol.* **398**, 353–363 (2005).